

# Learning the Boundary of Solvability: Aligning LLMs to Detect Unsolvable Problems

Dengyun Peng<sup>1,3\*</sup> Qiguang Chen<sup>1\*</sup> Bofei Liu<sup>1</sup> Jiannan Guan<sup>1</sup> Libo Qin<sup>2†</sup>  
 Zheng Yan<sup>1</sup> Jinhao Liu<sup>1</sup> Jianshu Zhang<sup>3</sup> Wanxiang Che<sup>1†</sup>

<sup>1</sup>LARG, Research Center for Social Computing and Interactive Robotics, HIT

<sup>2</sup>School of Computer Science and Engineering, Central South University

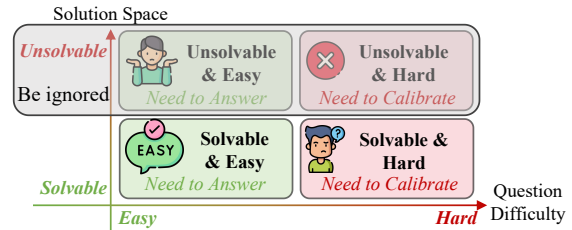
<sup>3</sup>iFLYTEK

## Abstract

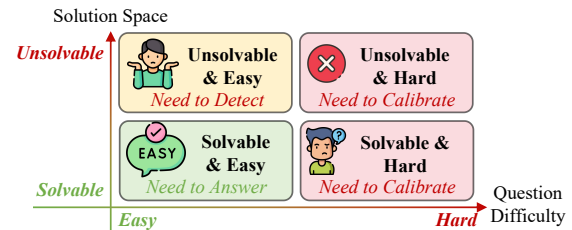
Ensuring LLM reliability requires not only solving complex problems but also recognizing when a problem is unsolvable. Current models often struggle to distinguish *objective unsolvability* (inherent contradictions in the problem) from *subjective capability limitations* (problems beyond the model’s competence), which leads to hallucinations and overconfidence. To address this, we propose UnsolvableQA and UnsolvableRL to solve feasible problems, detect inherent contradictions, and prudently refuse tasks beyond capability. Specifically, we construct **UnsolvableQA**, a dataset of paired solvable and unsolvable instances derived via a dual-track methodology: programmatic generation for logic puzzles and a novel “**Reverse Construction**” method that injects contradictions into valid reasoning chains for mathematics. Building on this dataset, we introduce UnsolvableRL, a reinforcement learning framework with three reward components jointly accounting for accuracy, unsolvability, and difficulty. Empirical results show that our approach achieves near-perfect unsolvability detection while also improving accuracy on solvable tasks. Crucially, we identify Capability Collapse, demonstrating that explicit exposure to unsolvable data is indispensable for preventing models from becoming systematically overconfident. Our code and data are available at <https://github.com/sfasfaffa/unsolvableQA>.

## 1 Introduction

As Large Language Models (LLMs) achieve strong performance on complex reasoning tasks (Chen et al., 2025c; Wei et al., 2022; Guo et al., 2025; Jaech et al., 2024), a key research direction (Qin et al., 2025) is ensuring they recognize their own limitations and behave reliably. Earlier work on confidence calibration (Xiong et al., 2023; Li et al.,



(a) Previous works about response based on Subjective Calibration.



(b) Response both based on Objective Detection and Subjective Calibration.

Figure 1: Comparison of alignment paradigms. We treat the solution space (solvable vs. unsolvable) and question difficulty (easy vs. hard) as orthogonal dimensions, requiring models to **objectively detect** contradictions and **subjectively calibrate** confidence.

2024; Yoon et al., 2025) and selective classification (Fisch et al., 2022) during reasoning underscores the need for models to know when not to answer. Further, studies on model **capability boundaries** (Chen et al., 2024) examine model self-awareness of their limitations to avoid unproductive reasoning on problems they are likely to fail (Zhang et al., 2025; Mei et al., 2025; Kalai et al., 2025; Chen et al., 2025b). More recently, TruthRL (Wei et al., 2025) encourages models to refuse when uncertain through a ternary reward mechanism.

However, a key limitation of these approaches is that they mainly focus on refusing questions that are *solvable but currently beyond the model’s capabilities* (“Need to Calibrate” region in Figure 1 (a)). This focus neglects a complementary and arguably more fundamental challenge: identifying problems that are *inherently unsolvable due to logical con-*

\*Equal contribution

†Corresponding Author

*traditions*. As illustrated by the gray “Be ignored” region in Figure 1 (a), existing models treat such an unsolvability as mere high difficulty or hallucinate answers even for simple contradictions.

To address this, our work distinguishes these scenarios by treating *Solution Space* (solvable vs. unsolvable) and *Question Difficulty* (easy vs. hard) as orthogonal dimensions (Figure 1 (b)). We argue that a reliable AI system must exhibit two behaviors: (1) **Objective Detection**, accurately identifying and flagging internally contradictory problems as “unsolvable” (top-left yellow quadrant); and (2) **Subjective Calibration**, safely refusing theoretically solvable problems that exceed the model’s current reasoning capacity. Without this distinction, models may confidently pursue hallucinations or unnecessarily reject solvable tasks.

First, to enable deep analysis of unsolvability, we present a fully automated pipeline and introduce **UnsolvableQA**, a dataset of paired solvable and unsolvable instances spanning logic, puzzles, and mathematics. For programmatically verifiable tasks, we create provably unsolvable instances by systematically injecting logical contradictions at the code level. For domains such as mathematics that lack direct programmatic verification, inspired by Lightman et al. (2024); Ling et al. (2023), we propose a “Reverse Construction” methodology. This LLM-driven approach starts from a solvable problem and its correct Chain-of-Thought (CoT), inserts a controlled logical contradiction into the CoT, and reverse-engineers a corresponding unsolvable problem aligned with the flawed reasoning.

To train models that remain robust on both solvable and unsolvable inputs, we design **UnsolvableRL**, a dynamic reward alignment scheme based on GRPO (Shao et al., 2024) that enables the model to detect *inherent* unsolvability and calibrate its confidence. Specifically, we assign distinct optimization objectives to two refusal types: (1) inherent unsolvability is formulated as a supervised classification task, whereas (2) capability-based calibration is governed by a dynamic confidence threshold with the model’s evolving performance.

Empirical results show a synergistic effect: UnsolvableRL achieves near-perfect precision in unsolvability detection and substantially higher reasoning accuracy on solvable tasks, nearly doubling the combined score. Our analysis also reveals a *capability collapse* phenomenon: without explicit exposure to unsolvable data, especially smaller models face a severe decline in self-monitoring,

becoming overconfident in their outputs.

Our contributions are summarized as follows:

- We propose a comprehensive alignment framework that treats objective unsolvability and subjective capability as orthogonal dimensions, establishing a robust three-way decision boundary for reliable reasoning.
- We introduce **UnsolvableQA**, a dataset constructed via a novel “Reverse Construction” methodology. This approach bridges the data gap by systematically injecting logical contradictions into valid Chain-of-Thought traces to generate verifiable unsolvable instances.
- We propose **UnsolvableRL**, a training paradigm leveraging dynamic confidence thresholds. This mechanism enables models to simultaneously learn to solve feasible tasks, detect inherent contradictions, and calibrate confidence on difficult problems.
- Empirical results demonstrate synergistic improvements in both detection and reasoning. Crucially, we identify the phenomenon of Capability Collapse, revealing that explicit unsolvable data is essential to prevent model overconfidence.

## 2 Related Work

There are two primary areas related to our work: automated dataset construction for reasoning and reinforcement learning approaches for incentivizing selective refusal.

As the reliance of Large Language Models on data quality increases, Automated Dataset Construction (ADC) has emerged as a prominent research direction (Liu et al., 2024; Wang et al., 2023). In the realm of reasoning, recent efforts primarily focus on ensuring data solvability and verifiability through formal or programmatic means. Representative works such as Enigmata (Chen et al., 2025a) and BIGGSM (Chen et al., 2024) have significantly enriched the resources for solvable reasoning tasks by employing synthetic puzzles and difficulty-graded annotations, respectively. Concurrently, research on verifying the correctness of Chain-of-Thought (CoT) traces has also been advancing (Ling et al., 2023; Chen et al., 2025c). In contrast, progress in dataset construction regarding problem unsolvability has been relatively slow.

Although earlier benchmarks like SQuAD 2.0 (Rajpurkar et al., 2018) attempted to include unanswerable questions, their task formats are overly simplistic (primarily extractive span selection) and fail to effectively evaluate the refusal capabilities of modern models in complex logical reasoning scenarios. Consequently, existing data synthesis efforts remain largely concentrated on *solvable* instances, leaving a significant research gap.

Beyond dataset construction, Reinforcement Learning (RL) (Ouyang et al., 2022; Schulman et al., 2017; Rafailov et al., 2024) has become a central approach for aligning LLMs with desired behaviors such as safety and truthfulness. Recent RL algorithms for reasoning, such as GRPO (Shao et al., 2024) and DAPO (Yu et al., 2025), further enhance models’ reasoning abilities (Sheng et al., 2025). Concurrent work also leverages RL to improve reasoning efficiency under cost constraints (Tu et al., 2025; Team et al., 2025; Guo et al., 2025; Wang et al., 2025; Chen et al., 2025b). In parallel, advances such as TruthRL (Wei et al., 2025) introduce objectives that encourage models to refuse likely hallucinations, and research on self-awareness enables models to decline answering when appropriate (Zhang et al., 2025; Mei et al., 2025; Kalai et al., 2025; Steyvers et al., 2025).

Despite these advancements, existing frameworks largely conflate *objective unsolvability* with *subjective uncertainty*. By focusing primarily on solvable instances or confidence calibration, they overlook the necessity of explicitly learning to identify logical contradictions. We bridge this gap by systematically constructing guaranteed-unsolvable data to enforce a robust three-way decision boundary: solving feasible tasks, detecting inherent unsolvability, and Calibrating Refusal for problems beyond the model’s current capabilities.

### 3 UnsolvabilityQA Construction

Existing benchmarks mainly target solvable tasks, leaving models prone to hallucinations when judging feasibility. To address this issue, we introduce UnsolvabilityQA, a dataset for detecting problem inherent contradictions.

To achieve this, we use a dual-track methodology (illustrated in Figure 2) tailored to the specific verification constraints of different domains.

#### 3.1 Mathematics Problem Generation via Reverse Construction

For mathematical reasoning tasks (e.g., algebra, geometry, combinatorics from AIME datasets), direct programmatic verification is often infeasible. We introduce a **Reverse Construction** methodology (see Figure 2 (a)) that leverages large language models to generate unsolvable problems by injecting logical contradictions into solvable seed problems, yielding high-quality unsolvable mathematics problems for training unsolvable policies.

Our reverse construction pipeline operates through two sequential stages:

**Data Generation Process:** First, we validate each seed problem by confirming that a strong reasoning model (DeepSeek-Reasoner) can correctly solve it and produce a complete chain-of-thought, ensuring sufficient reasoning capability. Then, we employ DeepSeek-Reasoner to design logical contradictions via two complementary strategies: *Constraint Contradiction*, which introduces conflicting external conditions, and *Axiom Contradiction*, which modifies reasoning steps to violate fundamental mathematical axioms. The model generates a structured plan specifying the location and mechanism of contradiction injection.

**Validation Process:** Based on this plan, the model then reverse-engineers a new problem statement that preserves the stylistic and complexity characteristics of the seed problem while embedding the designed contradiction. Finally, we implement a two-tier verification protocol: the generated problem is first presented to DeepSeek-Reasoner to autonomously detect contradictions; if this fails, we explicitly provide the contradiction plan to assess genuine unsolvability. Only instances passing verification are retained.

#### 3.2 Logic Puzzle Generation

To acquire strictly unsolvable questions in logic puzzle scenarios, we implement automated generators for four representative logic domains, following the sampling and verification process in Figure 2 (b). Each domain uses a deterministic solver to verify solutions and confirm unsolvability.

**Game24.** Solvability is checked by exhaustively enumerating all binary expression trees with exact rational arithmetic (Python Fraction) to avoid floating-point error. Unsolvable instances are obtained by *rejection sampling*, retaining number sets

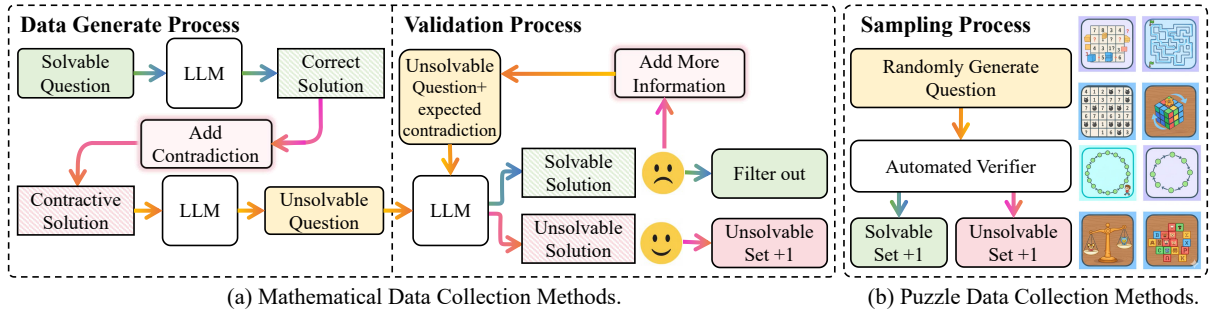


Figure 2: The **UnsolvableQA** data collection pipeline. **(a) Mathematical Data Collection:** We employ a “Reverse Construction” method where contradictions are injected into the solution path of solvable problems. The resulting instances are verified by an LLM to ensure they lead to a contradiction (unsolvable) rather than a valid solution. **(b) Puzzle Data Collection:** We utilize domain-specific programmatic generators and automated deterministic verifiers (e.g., SAT solvers, DFS) to rigorously classify randomly generated instances into solvable and unsolvable sets.

for which the exhaustive search proves that no solution exists.

**Hamiltonian Cycle/Path.** We encode graph traversability as a Boolean Satisfiability problem and verify randomly generated graphs using SAT solvers (MiniSat backend via pysat). Unsolvable instances are constructed by injecting structural impossibilities, such as removing critical edges to create bottlenecks or disconnecting components.

**Hitori.** We formulate Hitori as a Constraint Satisfaction Problem and, using python-constraint, generate puzzles with unique solutions. For unsolvable instances, we inject conflicting constraints, for example forcing a row or column to contain duplicate numbers that cannot be removed without violating adjacency rules.

**Maze Navigation.** Base mazes are generated via randomized Depth-First Search (DFS) to ensure nontrivial structure. To obtain unsolvable instances, we analyze all valid paths in a solvable maze and place an obstacle at a *critical junction* shared by every path, then verify unsolvability using Breadth-First Search (BFS).

### 3.3 Dataset Statistics and Quality Control

We construct UnsolvableQA to have approximately balanced solvable and unsolvable instances per domain, with minor residual imbalances caused by generator yields and verification constraints. Table 1 therefore reports aggregated statistics across the train and test partitions of **UnsolvableQA**. The test set contains 699 problems (358 solvable, 341 unsolvable), and the train set contains 637 problems (348 solvable, 289 unsolvable). The train partition pools all Maze instances without difficulty splits, whereas the test partition preserves

Split	Domain	Solvable	Unsolvable	Total
Train	Game24	50	50	100
Train	Hamiltonian Cycle	48	48	96
Train	Hamiltonian Path	50	50	100
Train	Hitori	50	50	100
Train	Maze	100	59	159
Train	AIME (1983–2023)	50	32	82
<hr/>				
Test	Game24	50	50	100
Test	Hamiltonian Cycle	48	50	98
Test	Hamiltonian Path	50	50	100
Test	Hitori	50	50	100
Test	Maze(Easy)	100	94	194
Test	AIME (2024–2025)	60	47	107
<hr/>				
Train Total	–	348	289	637
Test Total	–	358	341	699

Table 1: Unified vertical statistics for **UnsolvableQA** train/test partitions. Train Maze has no difficulty split; AIME year ranges differ. (Note: AIME year ranges: train 1983–2023; test 2024–2025.)

Maze Easy. The AIME partitions cover different year ranges. Test prompts are diversified and paraphrased, while train prompts follow templated formats for scalable generation. All instances pass automated quality-control checks: logic puzzles are verified with multiple SAT/CSP/graph solvers, maze and programmatic tasks with deterministic solvers, and mathematically constructed problems with multi-pass LLM-based verification.

## 4 UnsolvableRL Methodology

### 4.1 Problem Formulation

We formulate the reasoning task as generating a response  $y$  for a problem instance  $x$ , sampled from a distribution  $\mathcal{D}$ . Each instance  $x \in \mathcal{D}$  is either objectively solvable ( $x \in \mathcal{S}$ ) or unsolvable ( $x \in \mathcal{U}$ ), and is further categorized as subjectively easy ( $x \in \mathcal{E}$ ) or hard ( $x \in \mathcal{H}$ ).

Specifically, to satisfy three distinct behavioral objectives, our training framework optimizes a policy  $\pi_\theta$  as follows. First, for solvable and easy instances within the model’s capabilities ( $x \in \mathcal{S} \cap \mathcal{E}$ ), the objective is **Reasoning Accuracy**, requiring the model to produce correct reasoning chains and final answers. Second, for inherently unsolvable instances ( $x \in \mathcal{U} \cap \mathcal{E}$ ), the objective is **Unsolvability Detection**: the model must explicitly recognize the inconsistency and output a dedicated tag (e.g., <unsolvable>) instead of hallucinating a solution, which we treat as an *objective correctness* task. Third, for hard yet solvable instances ( $x \in \mathcal{H}$ ) that exceed the model’s effective reasoning capacity (as indicated by low internal confidence), the objective is **Capability Calibration**, where the model should prudently abstain (e.g., output <beyond\_capacity>) to reduce false positives.

## 4.2 Group-Relative Policy Optimization

To efficiently optimize the policy across heterogeneous objectives without training a separate value function, this work adopts Group Relative Policy Optimization (GRPO). For each input  $x$ , the policy samples a group of  $G$  outputs  $\mathcal{Y} = \{y_1, y_2, \dots, y_G\}$ . The optimization objective is defined as:

$$\mathcal{J}(\theta) = \mathbb{E}_{x, \mathcal{Y}} \left[ \frac{1}{G} \sum_{i=1}^G \min \left( r_i(\theta) A_i, \text{clip}(r_i(\theta), 1 - \epsilon, 1 + \epsilon) A_i \right) \right], \quad (1)$$

where  $r_i(\theta) = \frac{\pi_\theta(y_i|x)}{\pi_{\theta_{\text{old}}}(y_i|x)}$  is the probability ratio, and  $\epsilon$  is the clipping parameter. GRPO computes the advantage  $A_i$  for each output  $y_i$  by normalizing rewards within the group instead of using a critic model:

$$A_i = \frac{R(y_i | x) - \mu_{\mathbf{R}}}{\sigma_{\mathbf{R}} + \epsilon}, \quad (2)$$

where  $\mu_{\mathbf{R}}$  and  $\sigma_{\mathbf{R}}$  are the mean and standard deviation of the rewards  $\mathbf{R} = \{R(y_j | x)\}_{j=1}^G$  within the group. This group-based normalization can stabilize training due to reward-scale differences across solvable and unsolvable domains.

## 4.3 Reward Design

As illustrated in Figure 3, our framework explicitly distinguishes between three types of model responses: (1) **Reward for Reasoning Accuracy** (providing a solution), (2) **Reward for Unsolvability Detection** (identifying inherent contradictions),

and (3) **Reward for Capability Calibration** (admitting capability limits). We design a composite reward function that applies distinct mechanisms to these behaviors to align objective correctness with subjective capability.

**Reward for Reasoning Accuracy ( $R_{\text{acc}}$ ).** This component evaluates the correctness of the model’s judgments on verifiably solvable instances. (1) A *Correct Response* (+1) is assigned when the model outputs the correct answer for a solvable instance. (2) For *Incorrect Reasoning* (0) on solvable instances, such as producing an incorrect final answer despite performing the calculation, the model receives a neutral reward. This asymmetric scheme emphasizes reasoning capability by rewarding successful problem solving while not explicitly penalizing unsuccessful but genuine reasoning attempts on solvable tasks.

**Reward for Unsolvability Detection ( $R_{\text{detect}}$ ).** This component evaluates how accurately the model identifies inherently contradictory or ill-posed instances. (1) A *Correct-Detect Response* (+1) is assigned when the model explicitly outputs the canonical tag `unsolvable` for such an instance. (2) To prevent degenerate behavior, we impose a *False Unsolvability Penalty* ( $\rho = -0.5$ ): if the model incorrectly declares a solvable problem unsolvable, it receives a negative reward.

We explicitly motivate this penalty value via a decision-theoretic analysis (formal proof in Appendix A.1). Consider a model with an initial weak reasoning capability  $\epsilon$  on solvable tasks (e.g.,  $\epsilon \approx 0.1$ ) and a posterior belief  $p$  that a given problem is unsolvable. The model decides between two actions based on their expected rewards:

(1) **Attempting to Solve:** The expected reward depends on the problem being solvable and the model answering correctly:  $\mathbb{E}[\text{Attempt}] \approx (1 - p) \cdot \epsilon$ .

(2) **Declaring Unsolvable:** The expected reward is the weighted sum of a correct rejection and a false rejection penalty:  $\mathbb{E}[\text{Reject}] = p \cdot 1 + (1 - p) \cdot \rho$ .

The model will only attempt to reason if  $\mathbb{E}[\text{Attempt}] > \mathbb{E}[\text{Reject}]$ . Solving this inequality yields a critical threshold for the belief  $p$ :

$$p < \frac{\epsilon - \rho}{1 + \epsilon - \rho}$$

If we set  $\rho = 0$  (no penalty), the threshold collapses to  $p < 0.09$ , meaning the model refuses to answer unless it is over 91% sure the problem is solvable.

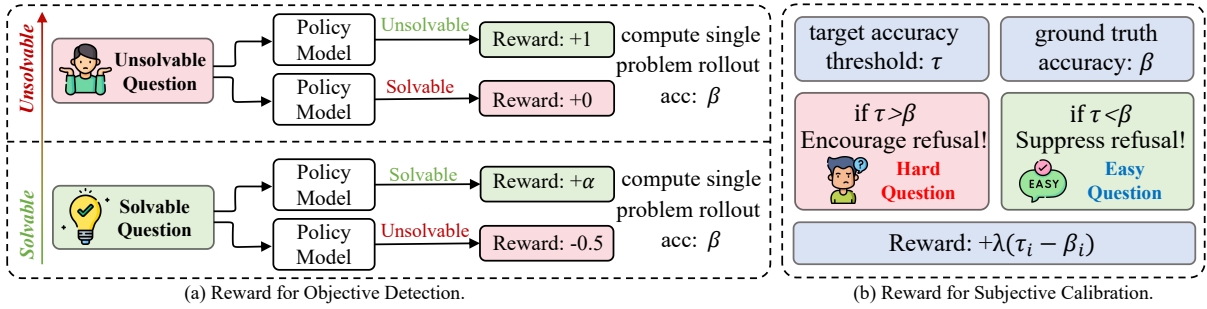


Figure 3: **UnsolvableRL Reward Framework.** We decompose the alignment into two orthogonal components: **(a) Objective Detection**, which incentivizes the model to distinguish between solvable and unsolvable queries. Crucially, we impose a penalty (-0.5) for falsely labeling solvable problems as unsolvable to safeguard the model’s reasoning drive. **(b) Subjective Calibration**, which dynamically regulates refusal behavior. By comparing the target threshold ( $\tau$ ) with the model’s rollout accuracy ( $\beta$ ), the mechanism encourages refusal on hard tasks (where  $\tau > \beta$ ) and suppresses it on easy ones (where  $\tau < \beta$ ) via the dynamic reward term  $\lambda(\tau_i - \beta_i)$ .

This leads to a local optimum of *universal rejection*. By setting  $\rho = -0.5$ , we relax this threshold to  $p < 0.375$ . This “Threshold Expansion” effectively encourages the model to attempt reasoning even under moderate uncertainty, preventing the collapse of reasoning capabilities.

(3) For *Error-Detect Reasoning* (0) on unsolvable instances, such as hallucinating a solution instead of outputting unsolvable, the model receives a neutral reward.

**Reward for Subjective Calibration ( $R_{\text{cal}}$ ).** When the model outputs the specific refusal token (e.g., beyond my capabilities), we do not apply a static score. Instead, we regulate refusal via a *target accuracy threshold*  $\tau \in [0, 1]$ . During each RL rollout, we compute the empirical accuracy  $\beta$  of the current group as:

$$\beta = \frac{1}{N} \sum_{i=1}^N \mathbf{1}[y_i \text{ is correct}], \quad (3)$$

where correctness includes both solving solvable problems and identifying unsolvable ones. The calibration reward is then defined as:

$$R_{\text{cal}}(y) = \lambda(\tau - \beta) \mathbf{1}[y \text{ is a refusal}]. \quad (4)$$

Here,  $(\tau - \beta)$  quantifies the *reliability deficit*—the gap between the target and the model’s actual performance. This creates a dynamic incentive mechanism as shown in Figure 3(b): when the model’s reasoning capability on the current batch is poor ( $\beta < \tau$ ), the term is positive, **encouraging refusal**; conversely, when performance is high ( $\beta > \tau$ ), the reward becomes negative, **suppressing refusal** on easy questions.

To enforce robust calibration, we implement a *progressive schedule* for  $\tau$ , increasing it steadily throughout training to approach 1. This curriculum balances exploration and caution: in early stages, a lower  $\tau$  provides a lenient margin to encourage the **exploration** of reasoning paths; in later stages, as  $\tau \rightarrow 1$ , it enforces a strict standard, compelling the model to answer **prudently**.

We mathematically justify the necessity of this dynamic schedule by analyzing the general condition for refusal. The model should choose to refuse only if the reward for refusal exceeds the expected reward of answering:

$$R_{\text{cal}} > \mathbb{E}[R_{\text{ans}}]. \quad (5)$$

Note that the expected reward for answering is always non-negative ( $\mathbb{E}[R_{\text{ans}}] \geq 0$ ). If we were to use a *fixed threshold* (e.g.,  $\tau = 0.5$ ), as the model’s reasoning capability improves, the batch accuracy  $\beta$  will likely surpass  $\tau$  (i.e.,  $\beta > \tau$ ). Once this occurs, the refusal reward becomes **negative** ( $R_{\text{cal}} < 0$ ). In this regime, the inequality  $R_{\text{cal}} > \mathbb{E}[R_{\text{ans}}]$  becomes impossible to satisfy, as a negative reward cannot exceed a non-negative one. Consequently, for well-performed batches, the model is incentivized to suppress refusal entirely to avoid penalties. Our progressive schedule prevents this collapse by ensuring  $\tau$  grows dynamically to maintain  $\tau \gtrsim \beta$ , keeping the refusal incentive positive for uncertain queries.

The final per-trajectory reward is the sum of these components:

$$R = R_{\text{acc}} + R_{\text{detect}} + R_{\text{cal}}. \quad (6)$$

	Game24			HamCycle			HamPath			Hitori			Maze(E)			AIME24-25			Overall		
	S	U	M	S	U	M	S	U	M	S	U	M	S	U	M	S	U	M	S	U	M
Qwen3-4B-Instruct	81.0	17.0	49.0	37.5	57.0	47.3	37.0	56.5	46.8	34.5	6.5	20.5	32.7	55.6	44.1	67.9	25.3	46.6	48.4	36.3	42.4
+ Solvable-Only	85.5	11.5	48.5	41.1	65.0	53.1	52.0	66.5	59.3	53.5	5.0	29.3	95.0	83.0	89.0	68.3	18.9	43.6	65.9	41.7	53.8
+ UnsolvbleRL-Mid	84.5	98.5	91.5	36.5	95.5	66.0	44.0	98.0	71.0	47.0	72.5	59.8	95.7	94.9	95.3	67.3	52.7	60.0	62.5	85.4	73.9
+ Fixed- $\tau$	85.5	99.0	92.3	43.8	99.5	71.6	59.5	99.0	79.3	48.5	98.0	73.3	96.6	99.5	98.0	69.6	61.4	65.5	67.3	92.7	80.0
+ UnsolvbleRL-Final	92.0	99.0	95.5	41.1	94.5	67.8	55.0	96.5	75.8	63.5	94.5	79.0	96.0	98.9	97.5	69.2	85.0	77.1	69.5	90.9	80.3
Qwen3-1.7B-Instruct	63.0	21.0	42.0	22.9	22.5	22.7	13.0	26.5	19.8	6.0	27.0	16.5	3.6	91.0	47.3	38.3	37.5	37.9	24.5	37.6	31.0
+ Solvable-Only	78.5	1.0	39.8	23.4	2.0	12.7	13.5	2.5	8.0	4.5	1.5	3.0	5.7	0.0	2.9	41.7	2.1	21.9	27.9	1.5	14.7
+ UnsolvbleRL-Mid	70.5	90.5	80.5	19.3	85.5	52.4	17.0	91.5	54.3	11.0	56.0	33.5	4.1	92.0	48.1	39.2	39.6	39.4	26.9	75.9	51.4
+ UnsolvbleRL-Final	79.0	99.5	89.3	21.9	87.5	54.7	17.0	87.5	52.3	6.0	56.5	31.3	8.6	96.8	52.7	37.3	48.4	42.8	28.3	79.4	53.9

Table 2: Per-domain performance for Qwen3 checkpoints. Values are percentages. For each test domain we report solvable accuracy (S), unsolvable rejection rate (U), and their mean ( $M = (S+U)/2$ ). Overall metrics are unweighted means across all 6 domains. Model names indicate the training configuration and stage: **UnsolvbleRL** is our main method trained on paired solvable/unsolvable data; **Solvable-Only** is an ablation trained exclusively on solvable instances (Step 60 for 1.7B, Step 120 for 4B); **Fixed- $\tau$**  is an ablation using a fixed calibration threshold. Suffixes **Mid** and **Final** represent intermediate (Step 60 for 1.7B, Step 120 for 4B) and extended (Step 360 for 1.7B, Step 320 for 4B) trained models, respectively.

Checkpoint	Game24			HamCycle			HamPath			Hitori			Maze(E)			AIME24-25			Overall		
	Corr	Rej	C+R	Corr	Rej	C+R	Corr	Rej	C+R	Corr	Rej	C+R	Corr	Rej	C+R	Corr	Rej	C+R	Corr	Rej	C+R
Qwen3-4B-Instruct	49.0	0.00	49.0	47.3	24.74	72.0	46.8	12.00	58.8	20.5	4.00	24.5	44.1	0.00	44.1	46.6	0.00	46.6	42.4	6.79	49.2
+ Solvable-Only	48.5	0.00	48.5	53.1	20.57	73.7	59.3	7.50	66.8	29.3	1.50	30.8	89.0	0.00	89.0	43.6	0.00	43.6	53.8	4.93	58.7
+ UnsolvbleRL-Mid	91.5	0.00	91.5	66.0	19.01	85.0	71.0	13.00	84.0	59.8	1.50	61.3	95.3	0.00	95.3	60.0	0.00	60.0	73.9	5.59	79.5
+ Fixed- $\tau$	92.3	0.00	92.3	71.6	17.19	88.8	79.3	10.00	89.3	73.3	1.00	74.3	98.0	0.00	98.0	65.5	0.00	65.5	80.0	4.70	84.7
+ UnsolvbleRL-Final	95.5	0.00	95.5	67.8	26.82	94.6	75.8	19.00	94.8	79.0	2.25	81.3	97.5	0.00	97.5	65.9	0.00	65.9	80.3	8.01	88.3
Qwen3-1.7B-Instruct	42.0	0.00	42.0	22.7	9.38	32.1	19.8	9.25	29.0	16.5	0.50	17.0	47.3	0.00	47.3	37.9	0.21	38.1	31.0	3.22	34.3
+ Solvable-Only	39.8	0.00	39.8	12.7	10.94	23.6	8.0	7.00	15.0	3.0	0.25	3.3	2.9	0.00	2.9	21.9	0.10	22.0	14.7	3.05	17.8
+ UnsolvbleRL-Mid	80.5	0.00	80.5	52.4	21.35	73.8	54.3	13.00	67.3	33.5	2.00	35.5	48.1	0.00	48.1	39.4	2.08	41.5	51.4	6.41	57.8
+ UnsolvbleRL-Final	89.3	0.25	89.6	54.7	23.44	78.1	52.3	18.00	70.3	31.3	1.75	33.0	52.7	0.00	52.7	42.8	1.88	44.7	53.9	7.55	61.4

Table 3: Aggregated domain-level metrics for Qwen3 checkpoints. Each domain reports: Correctness (mean of solvable and unsolvable correct rates), Rejection (mean rejection rate), and Combined = Correctness + Rejection. Overall columns are unweighted means across domains.

#### 4.4 Answer Extraction and Verification

For solvable tasks, deterministic verifiers (graph and constraint solvers, arithmetic evaluators, and reference-answer matchers) are applied. For unsolvable tasks, verification instead checks for the canonical unsolvable marker. For logic puzzles, domain-specific verifiers check the extracted answer against problem constraints and ground-truth solutions. For AIME and other mathematics problems, “math\_verify” is used for symbolic equivalence checking. Answers containing “beyond my capabilities” are treated as calibration and handled by the dynamic reward logic.

### 5 Experiments

We evaluated Qwen3-1.7B and Qwen3-4B (Yang et al., 2025) with think mode after training and testing on UnsolvbleQA. For evaluation, we report average@8 on the AIME solvable and unsolvable partitions to account for higher variance, and average@4 on all other datasets.

**UnsolvbleRL substantially improves both accuracy and calibration.** As shown in Table 3, fine-tuning on a mixture of solvable and unsolvable

data yields a consistent increase in overall accuracy across all test sets for both models. Aggregated metrics indicate that Qwen3-4B’s combined performance score (C+R) increases from 49.2% to 88.3% under the UnsolvbleRL-Final configuration. Crucially, UnsolvbleRL significantly improves unsolvable detection capabilities: the mean rejection rate on unsolvable instances ( $U_{\text{mean}}$ ) surged from 36.3% to 90.9% for Qwen3-4B, and from 37.6% to 79.4% for Qwen3-1.7B. In complex reasoning domains such as Game24 and Hamiltonian Path, the model attains rejection rates above 94% on unsolvable instances while maintaining, and in some cases improving, performance on solvable ones; for example, solvable accuracy on Game24 improves from 81.0% to 92.0%. Together, these results demonstrate that our training methodology enables the models to reliably distinguish between solvable and unsolvable problems and to exhibit the desired behavior of either answering correctly or abstaining.

**Training on solvable-only data is fundamentally insufficient for learning robust calibration.** We further conducted an ablation study by training

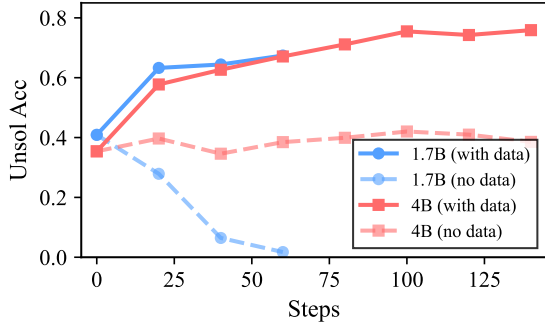


Figure 4: Evolution of Unsolvable Accuracy during training. The curves represent the average detection accuracy across unsolvable instances from the evaluated domains. Models trained with **UnsolvableQA** (solid lines) steadily improve their ability to identify contradictions. In contrast, the “No Data” ablation (dashed lines) leads to stagnation or, specifically for the 1.7B model, a catastrophic collapse in unsolvability detection.

models on a variant of our data with all unsolvable instances removed (Solvable-Only). We compare the Solvable-Only model with the full-training (UnsolvableRL) model at the same RL steps. As shown in Table 2, the Qwen3-1.7B-Solvable-Only model’s mean unsolvable rejection rate collapses to 1.5%, compared to 75.9% for the UnsolvableRL model. This catastrophic failure underscores the necessity of explicitly including unsolvable examples during training to prevent over-confidence.

### Dynamic thresholds achieve a more favorable trade-off between performance and calibration.

To assess the effectiveness of the Reward for Subjective Calibration, we compare our main model with a **Fixed- $\tau$**  variant that uses a static low threshold. As shown in Table 3, the dynamic mechanism substantially increases refusal under uncertainty, raising the mean rejection rate on solvable instances from 4.70% (Fixed- $\tau$ ) to 8.01%. This behavior arises from the interaction between model capability and reward. As training progresses and the model’s reasoning capability improves, the empirical accuracy  $\beta$  increases. Under Fixed- $\tau$ , once performance exceeds the static threshold ( $\beta > \tau$ ), the calibration reward term  $\lambda(\tau - \beta)$  becomes negative, penalizing refusal and effectively forcing the model to hallucinate answers on difficult problems. In contrast, our dynamic mechanism adjusts  $\tau$  based on  $\beta$ , maintaining a positive incentive for refusal only when necessary. We provide a formal proof of this *Capability-Refusal Trade-off* in Appendix A.2. Consequently, the dynamic approach

achieves a better balance, maintaining strong accuracy (Overall  $S$  of 69.5% vs. 67.3%) alongside safer behavior.

### Training without unsolvable instances leads to the collapse of unsolvability detection.

To further assess the role of negative supervision, we analyze the training dynamics in Figure 4. We track the *Unsolvable Accuracy*, defined as the accuracy of detecting unsolvable instances averaged across our evaluation domains. Models trained with our paired data (solid lines) steadily improve at detecting inherent contradictions, whereas ablation models without unsolvable samples (dashed lines) fail to generalize. This gap is most pronounced in the 1.7B model, which exhibits a sharp **capability collapse**, with its accuracy on unsolvable problems approaching zero. We attribute this to *Gradient Interference* in smaller models, where optimization for answering solvable questions suppresses the features required for detection (see Appendix A.3 for a theoretical derivation). These results demonstrate that explicit exposure to unsolvable problems is crucial for preventing overconfidence.

## 6 Conclusion

In this paper, we enhance the reliability of large language models (LLMs) by introducing two novel perspectives: detecting inherently unsolvable problems and calibrating model behavior on problems beyond their capabilities. To this end, we construct UnsolvableQA using a novel Reverse Construction methodology and align models with UnsolvableRL, which incorporates a dynamic refusal mechanism. Our approach enables models to effectively refuse both unsolvable and highly uncertain queries without degrading their reasoning performance. We expect this work to advance the development of LLMs that understand not only how to solve problems, but also when not to attempt them.

## 7 Future Work

We plan to extend this work in three directions. First, we will construct diverse Out-of-Distribution (OOD) test sets to rigorously assess the generalization of refusal boundaries. Second, we aim to empirically investigate the root cause of Capability Collapse in smaller models, verifying our gradient interference hypothesis via feature space analysis. Finally, we will validate the scalability of our framework by applying it to a broader range of model architectures.

## References

- Jiangjie Chen, Qianyu He, Siyu Yuan, Aili Chen, Zhicheng Cai, Weinan Dai, Hongli Yu, Qiyang Yu, Xuefeng Li, Jiaye Chen, and 1 others. 2025a. Enigmata: Scaling logical reasoning in large language models with synthetic verifiable puzzles. *arXiv preprint arXiv:2505.19914*.
- Qiguang Chen, Dengyun Peng, Jinhao Liu, HuiKang Su, Jiannan Guan, Libo Qin, and Wanxiang Che. 2025b. Aware first, think less: Dynamic boundary self-awareness drives extreme reasoning efficiency in large language models. *arXiv preprint arXiv:2508.11582*.
- Qiguang Chen, Libo Qin, Jinhao Liu, Dengyun Peng, Jiannan Guan, Peng Wang, Mengkang Hu, Yuhang Zhou, Te Gao, and Wanxiang Che. 2025c. Towards reasoning era: A survey of long chain-of-thought for reasoning large language models. *arXiv preprint arXiv:2503.09567*.
- Qiguang Chen, Libo Qin, Jiaqi Wang, Jingxuan Zhou, and Wanxiang Che. 2024. Unlocking the capabilities of thought: A reasoning boundary framework to quantify and optimize chain-of-thought. *Advances in Neural Information Processing Systems*, 37:54872–54904.
- Adam Fisch, Tommi Jaakkola, and Regina Barzilay. 2022. Calibrated selective classification. *arXiv preprint arXiv:2208.12084*.
- Daya Guo, Dejian Yang, Haowei Zhang, Junxiao Song, Ruoyu Zhang, Runxin Xu, Qihao Zhu, Shitong Ma, Peiyi Wang, Xiao Bi, and 1 others. 2025. Deepseek-r1: Incentivizing reasoning capability in llms via reinforcement learning. *arXiv preprint arXiv:2501.12948*.
- Aaron Jaech, Adam Kalai, Adam Lerer, Adam Richardson, Ahmed El-Kishky, Aiden Low, Alec Helyar, Aleksander Madry, Alex Beutel, Alex Carney, and 1 others. 2024. Openai o1 system card. *arXiv preprint arXiv:2412.16720*.
- Adam Tauman Kalai, Ofir Nachum, Santosh S. Vempala, and Edwin Zhang. 2025. [Why language models hallucinate](#). *Preprint*, arXiv:2509.04664.
- Loka Li, Zhenhao Chen, Guangyi Chen, Yixuan Zhang, Yusheng Su, Eric Xing, and Kun Zhang. 2024. Confidence matters: Revisiting intrinsic self-correction capabilities of large language models. *arXiv preprint arXiv:2402.12563*.
- Hunter Lightman, Vineet Kosaraju, Yuri Burda, Harrison Edwards, Bowen Baker, Teddy Lee, Jan Leike, John Schulman, Ilya Sutskever, and Karl Cobbe. 2024. Let’s verify step by step. In *The Twelfth International Conference on Learning Representations*.
- Zhan Ling, Yunhao Fang, Xuanlin Li, Zhiao Huang, Mingu Lee, Roland Memisevic, and Hao Su. 2023. Deductive verification of chain-of-thought reasoning. *Advances in Neural Information Processing Systems*, 36:36407–36433.
- Minghao Liu, Zonglin Di, Jiaheng Wei, Zhongruo Wang, Hengxiang Zhang, Ruixuan Xiao, Haoyu Wang, Jintong Pang, Hao Chen, Ankit Shah, and 1 others. 2024. Automatic dataset construction (adc): Sample collection, data curation, and beyond. *arXiv preprint arXiv:2408.11338*.
- Zhiting Mei, Christina Zhang, Tenny Yin, Justin Lillard, Ola Shorinwa, and Anirudha Majumdar. 2025. Reasoning about uncertainty: Do reasoning models know when they don’t know? *arXiv preprint arXiv:2506.18183*.
- Long Ouyang, Jeff Wu, Xu Jiang, Diogo Almeida, Carroll L. Wainwright, Pamela Mishkin, Chong Zhang, Sandhini Agarwal, Katarina Slama, Alex Ray, John Schulman, Jacob Hilton, Fraser Kelton, Luke Miller, Maddie Simens, Amanda Askell, Peter Welinder, Paul Christiano, Jan Leike, and Ryan Lowe. 2022. [Training language models to follow instructions with human feedback](#). *Preprint*, arXiv:2203.02155.
- Libo Qin, Qiguang Chen, Xiachong Feng, Yang Wu, Yongheng Zhang, Yinghui Li, Min Li, Wanxiang Che, and Philip S. Yu. 2025. [Large language models meet nlp: A survey](#). *Preprint*, arXiv:2405.12819.
- Rafael Rafailov, Archit Sharma, Eric Mitchell, Stefano Ermon, Christopher D. Manning, and Chelsea Finn. 2024. [Direct preference optimization: Your language model is secretly a reward model](#). *Preprint*, arXiv:2305.18290.
- Pranav Rajpurkar, Robin Jia, and Percy Liang. 2018. [Know what you don’t know: Unanswerable questions for squad](#). *Preprint*, arXiv:1806.03822.
- John Schulman, Filip Wolski, Prafulla Dhariwal, Alec Radford, and Oleg Klimov. 2017. [Proximal policy optimization algorithms](#). *Preprint*, arXiv:1707.06347.
- Zhihong Shao, Peiyi Wang, Qihao Zhu, Runxin Xu, Junxiao Song, Xiao Bi, Haowei Zhang, Mingchuan Zhang, YK Li, Yang Wu, and 1 others. 2024. Deepseekmath: Pushing the limits of mathematical reasoning in open language models. *arXiv preprint arXiv:2402.03300*.
- Guangming Sheng, Chi Zhang, Zilingfeng Ye, Xibin Wu, Wang Zhang, Ru Zhang, Yanghua Peng, Haibin Lin, and Chuan Wu. 2025. Hybridflow: A flexible and efficient rlhf framework. In *Proceedings of the Twentieth European Conference on Computer Systems*, pages 1279–1297.
- Mark Steyvers, Heliodoro Tejada, Aakriti Kumar, Catarina Belem, Sheer Karny, Xinyue Hu, Lukas W. Mayer, and Padhraic Smyth. 2025. [What large language models know and what people think they know](#). *Nature Machine Intelligence*, 7(2):221–231.

- Kimi Team, Angang Du, Bofei Gao, Bowei Xing, Changjiu Jiang, Cheng Chen, Cheng Li, Chenjun Xiao, Chenzhuang Du, Chonghua Liao, and 1 others. 2025. Kimi k1.5: Scaling reinforcement learning with llms. *arXiv preprint arXiv:2501.12599*.
- Songjun Tu, Jiahao Lin, Qichao Zhang, Xiangyu Tian, Linjing Li, Xiangyuan Lan, and Dongbin Zhao. 2025. Learning when to think: Shaping adaptive reasoning in r1-style models via multi-stage rl. *arXiv preprint arXiv:2505.10832*.
- Jiakang Wang, Runze Liu, Lei Lin, Wenping Hu, Xiu Li, Fuzheng Zhang, Guorui Zhou, and Kun Gai. 2025. [Aspo: Asymmetric importance sampling policy optimization](#). *Preprint*, arXiv:2510.06062.
- Zige Wang, Wanjun Zhong, Yufei Wang, Qi Zhu, Fei Mi, Baojun Wang, Lifeng Shang, Xin Jiang, and Qun Liu. 2023. Data management for training large language models: A survey. *arXiv preprint arXiv:2312.01700*.
- Jason Wei, Xuezhi Wang, Dale Schuurmans, Maarten Bosma, Fei Xia, Ed Chi, Quoc V Le, Denny Zhou, and 1 others. 2022. Chain-of-thought prompting elicits reasoning in large language models. *Advances in neural information processing systems*, 35:24824–24837.
- Zhepei Wei, Xiao Yang, Kai Sun, Jiaqi Wang, Rulin Shao, Sean Chen, Mohammad Kachuee, Teja Gollapudi, Tony Liao, Nicolas Scheffer, and 1 others. 2025. Truthrl: Incentivizing truthful llms via reinforcement learning. *arXiv preprint arXiv:2509.25760*.
- Miao Xiong, Zhiyuan Hu, Xinyang Lu, Yifei Li, Jie Fu, Junxian He, and Bryan Hooi. 2023. Can llms express their uncertainty? an empirical evaluation of confidence elicitation in llms. *arXiv preprint arXiv:2306.13063*.
- An Yang, Anfeng Li, Baosong Yang, Beichen Zhang, Binyuan Hui, Bo Zheng, Bowen Yu, Chang Gao, Chengen Huang, Chenxu Lv, Chujie Zheng, Dayiheng Liu, Fan Zhou, Fei Huang, Feng Hu, Hao Ge, Haoran Wei, Huan Lin, Jialong Tang, and 41 others. 2025. [Qwen3 technical report](#). *Preprint*, arXiv:2505.09388.
- Dongkeun Yoon, Seungone Kim, Sohee Yang, Sunkyoung Kim, Soyeon Kim, Yongil Kim, Eunbi Choi, Yireun Kim, and Minjoon Seo. 2025. Reasoning models better express their confidence. *arXiv preprint arXiv:2505.14489*.
- Qiyang Yu, Zheng Zhang, Ruofei Zhu, Yufeng Yuan, Xiaochen Zuo, Yu Yue, Weinan Dai, Tiantian Fan, Gaohong Liu, Lingjun Liu, Xin Liu, Haibin Lin, Zhiqi Lin, Bole Ma, Guangming Sheng, Yuxuan Tong, Chi Zhang, Mofan Zhang, Wang Zhang, and 16 others. 2025. [Dapo: An open-source llm reinforcement learning system at scale](#). *Preprint*, arXiv:2503.14476.
- Qingjie Zhang, Yujia Fu, Yang Wang, Liu Yan, Tao Wei, Ke Xu, Minlie Huang, and Han Qiu. 2025. On the self-awareness of large reasoning models’ capability boundaries. *arXiv preprint arXiv:2509.24711*.

## A Appendix

### A.1 Theoretical Justification for False Unsolvability Penalty

In this section, we provide a theoretical derivation to demonstrate why the penalty  $\rho = -0.5$  is critical for preventing reward hacking, specifically the phenomenon of “collapse to universal rejection.”

**Problem Setup.** Let  $x$  be an input problem. Let  $\mathcal{S}$  and  $\mathcal{U}$  denote the sets of solvable and inherently unsolvable problems, respectively. Based on our dataset distribution, we assume balanced prior probabilities  $P(x \in \mathcal{S}) = P(x \in \mathcal{U}) = 0.5$ . Let the model have a weak initial reasoning capability  $\epsilon$  on solvable tasks (e.g.,  $\epsilon \approx 0.1$ ), meaning the probability of generating a correct solution given a solvable attempt is  $P(\text{correct} \mid x \in \mathcal{S}, \text{attempt}) = \epsilon$ . Conversely, identifying unsolvability is a binary decision: if the model predicts “unsolvable”, it receives a reward of  $+1$  if  $x \in \mathcal{U}$  and a penalty  $\rho$  if  $x \in \mathcal{S}$  (False Unsolvability).

**Decision Analysis.** Consider the model’s decision process for a given input  $x$  where the model has a posterior belief  $p = P(x \in \mathcal{U})$  that the problem is unsolvable. The model compares the expected rewards  $\mathbb{E}[R]$  of two actions: Attempting to Solve versus Rejecting.

For the **Attempt** action, the model tries to generate a solution. The expected reward is the probability the problem is solvable multiplied by the success rate  $\epsilon$ :

$$\mathbb{E}[R_{\text{attempt}}] = (1 - p) \cdot \epsilon \cdot (+1) + p \cdot 0 = (1 - p)\epsilon. \quad (7)$$

Note that attempting to solve an inherently unsolvable problem yields 0 reward (hallucination).

For the **Reject** action, the model outputs “unsolvable”. The expected reward is the probability the problem is truly unsolvable plus the penalty for a false rejection:

$$\mathbb{E}[R_{\text{reject}}] = p \cdot (+1) + (1 - p) \cdot \rho. \quad (8)$$

**The Attempt Threshold.** The model will choose to *Attempt* only when  $\mathbb{E}[R_{\text{attempt}}] > \mathbb{E}[R_{\text{reject}}]$ . Substituting the values, we get  $(1 - p)\epsilon > p + (1 - p)\rho$ . Solving for  $p$ , we derive the critical condition for attempting reasoning:

$$p < \frac{\epsilon - \rho}{1 + \epsilon - \rho}. \quad (9)$$

This inequality defines the *Attempt Threshold*  $T$ . The model attempts reasoning only if its suspicion of unsolvability  $p$  is lower than  $T$ .

**Case 1: No Penalty ( $\rho = 0$ ).** Substituting  $\epsilon = 0.1$  and  $\rho = 0$ , we get  $T_{\text{zero}} = \frac{0.1}{1+0.1} \approx 0.09$ . This implies the model will only attempt to solve if it is more than **91% sure** the problem is solvable. Given the uncertainty in early training stages (where  $p$  is often near 0.5), the condition  $p < 0.09$  is rarely met. The optimal strategy collapses to “**Always Reject**”, as it guarantees a risk-free average reward of 0.5 (since 50% of data is unsolvable) compared to the meager 0.05 expected from attempting.

**Case 2: With Penalty ( $\rho = -0.5$ ).** Substituting  $\epsilon = 0.1$  and  $\rho = -0.5$ , we get  $T_{\text{penalty}} = \frac{0.1 - (-0.5)}{1 + 0.1 - (-0.5)} = \frac{0.6}{1.6} = 0.375$ . The threshold expands significantly from 0.09 to 0.375 (a  $4\times$  increase). The model becomes willing to attempt reasoning even when it has moderate uncertainty about the problem’s solvability. This negative constraint effectively counteracts the low initial reasoning accuracy, forcing the model to explore solvable paths rather than collapsing into the local optimum of universal rejection.

### A.2 Theoretical Analysis of Capability-Refusal Dynamics

In this section, we derive the mathematical relationship between the model’s reasoning capability and its tendency to refuse, explaining why a dynamic threshold is essential for preventing hallucination as the model becomes stronger.

**Decision Model.** For a given solvable input  $x$ , let the model’s internal confidence (probability of generating the correct answer) be  $p_{\text{correct}}$ . The model chooses between two actions: *Answer* or *Refuse*. The expected reward for answering is:

$$\mathbb{E}[R_{\text{answer}}] = p_{\text{correct}} \cdot (+1) + (1 - p_{\text{correct}}) \cdot 0 = p_{\text{correct}} \quad (10)$$

The expected reward for refusing is determined by the current batch accuracy  $\beta$  and the target threshold  $\tau$ :

$$\mathbb{E}[R_{\text{refuse}}] = \lambda(\tau - \beta) \quad (11)$$

The model will choose to **Refuse** only if the expected reward of refusing exceeds that of answering:

$$\lambda(\tau - \beta) > p_{\text{correct}} \quad \implies \quad p_{\text{correct}} < \lambda(\tau - \beta) \quad (12)$$

**Dynamics under Training.** During the training process, the model’s reasoning capability improves, which leads to two simultaneous changes: 1. For a specific difficult problem, the model’s confidence  $p_{\text{correct}}$  increases. 2. The overall batch accuracy  $\beta$  increases as the model solves more easy/medium problems correctly.

**Failure of Fixed Threshold (Fixed- $\tau$ ).** If we fix the threshold  $\tau$  to a constant value (e.g.,  $\tau = 0.5$ ), as the model converges, the batch accuracy  $\beta$  will likely surpass  $\tau$  (i.e.,  $\beta > \tau$ ). When  $\beta > \tau$ , the term  $\lambda(\tau - \beta)$  becomes **negative**. Substituting this into Inequality 12, the condition becomes:

$$p_{\text{correct}} < \text{Negative Value} \quad (13)$$

Since probability  $p_{\text{correct}} \in [0, 1]$  is always non-negative, this condition is **impossible to satisfy**. Therefore, the model will *never* refuse, even if its confidence  $p_{\text{correct}}$  is extremely low (e.g., 0.01). It is forced to hallucinate an answer to avoid the penalty of refusal. This explains the lower rejection rate and lower accuracy observed in the Fixed- $\tau$  experiments.

**Success of Dynamic Threshold.** By dynamically setting  $\tau$  (e.g., slightly higher than the moving average of  $\beta$ ), we ensure that  $(\tau - \beta)$  remains positive or near-zero. This maintains a valid decision boundary on the right side of Inequality 12, allowing the model to rationally refuse when its confidence  $p_{\text{correct}}$  is truly low, regardless of how strong the model becomes overall.

### A.3 Theoretical Analysis of Capability Collapse in Small Models

In this section, we propose a theoretical hypothesis for the *capability collapse* observed in smaller models (e.g., 1.7B) under the “No Data” setting. We frame this phenomenon as a potential instance of **Gradient Interference** arising from shared feature representations.

**Problem Definition.** Let  $x$  be an input problem. We define the model’s refusal policy via a scalar logit  $h_{\theta}(x) = w^{\top} \phi(x)$ , where  $\phi(x)$  represents the features in the last hidden layer and  $w$  is the weight vector of the refusal classification head. The probability of rejection is  $P(\text{reject}|x) = \sigma(h_{\theta}(x))$ .

**Training Dynamics under “No Data”.** In the ablation setting, the training set  $\mathcal{D}_{\text{train}}$  contains only solvable problems ( $x_s \in \mathcal{S}$ ). The objective is to maximize the probability of answering (accepting) these problems. The loss function for a solvable sample  $x_s$  can be formulated as minimizing the negative log-likelihood of not rejecting:

$$\mathcal{L}(\theta) = -\log(1 - P(\text{reject}|x_s)) = -\log(1 - \sigma(w^{\top} \phi(x_s))) \quad (14)$$

Computing the gradient with respect to  $w$ , we obtain:

$$\nabla_w \mathcal{L} = \frac{1}{1 - \sigma} \cdot \frac{\partial(1 - \sigma)}{\partial h} \cdot \phi(x_s) = \sigma(w^{\top} \phi(x_s)) \cdot \phi(x_s) = P(\text{reject}|x_s) \cdot \phi(x_s) \quad (15)$$

Assuming simplified SGD with learning rate  $\alpha$ , the weight update is:

$$\Delta w \propto -\nabla_w \mathcal{L} = -\alpha \cdot P(\text{reject}|x_s) \cdot \phi(x_s) \quad (16)$$

Intuitively, whenever the model assigns a non-zero probability to rejecting a solvable problem (a false rejection), the optimizer pushes the weight vector  $w$  in the direction opposite to  $\phi(x_s)$  to suppress this behavior.

**Hypothesized Impact on Unsolvable Test Data.** Consider an unsolvable test instance  $x_u \in \mathcal{U}$ . The resulting change in its refusal logit  $h(x_u)$  would be:

$$\Delta h(x_u) = (\Delta w)^{\top} \phi(x_u) \propto -\alpha \cdot P(\text{reject}|x_s) \cdot \left( \phi(x_s)^{\top} \phi(x_u) \right) \quad (17)$$

---

**Algorithm 1** Game24 Generation and Verification

---

**Require:** Difficulty level  $D$  (determines count  $k \in \{4, 5, 6\}$ ), Target  $T = 24$

**Ensure:** A paired instance  $(S, \text{Label})$

```
1: Function VERIFY( $S$ ):
2:    $\mathcal{T} \leftarrow$  All binary expression trees for set  $S$ 
3:   for each tree  $t \in \mathcal{T}$  do
4:     Evaluate  $val \leftarrow t$  using Rational Arithmetic
5:     if  $val == T$  then return SOLVABLE,  $t$ 
6:   end for
7:   return UNSOLVABLE,  $\emptyset$ 
8: End Function
9: repeat
10:  Sample a set of  $k$  integers  $S \leftarrow \{n_1, \dots, n_k\}$  where  $n_i \in [1, 13]$ 
11:   $Status, Proof \leftarrow$  VERIFY( $S$ )
12:  if goal is Solvable and  $Status ==$  SOLVABLE:
13:    return ( $S, Proof$ )
14:  else if goal is Unsolvable and  $Status ==$  UNSOLVABLE:
15:    return ( $S, \text{"Unsolvable"}$ )
16: until Valid instance found
```

---

This derivation suggests that the impact on unsolvable instances depends critically on the geometric relationship between the feature representations of solvable and unsolvable problems:

- **High Capacity Models (e.g., 4B+):** We hypothesize that larger models can learn distinct, nearly orthogonal representations for solvable versus inherently contradictory problems (i.e.,  $\phi(x_s)^\top \phi(x_u) \approx 0$ ). In this case, suppressing rejection on  $x_s$  has minimal impact on the model’s ability to reject  $x_u$ .
- **Low Capacity Models (e.g., 1.7B):** Smaller models may suffer from feature entanglement, relying on shared heuristics (such as sentence complexity or topic) to represent both problem types. If  $\phi(x_s)$  and  $\phi(x_u)$  are positively correlated ( $\phi(x_s)^\top \phi(x_u) > 0$ ), the term  $\Delta h(x_u)$  becomes negative.

**Conclusion.** Under the assumption of feature entanglement in smaller models, training to answer solvable questions implicitly generates a negative gradient for the refusal logits of unsolvable questions. Without explicit negative samples ( $x_u$ ) in the training set to provide a counter-gradient, this interference likely drives the refusal probability for unsolvable data toward zero, resulting in the observed capability collapse.

## A.4 Logic Puzzle Generation Algorithms

### A.4.1 Game24 Generation

The Game24 task involves combining a set of integers using arithmetic operations ( $+$ ,  $-$ ,  $\times$ ,  $\div$ ) to equal 24. To ensure absolute correctness, particularly for unsolvable instances, we employ an exhaustive search over all possible binary expression trees. Crucially, we utilize exact rational arithmetic (e.g., Python’s Fraction) rather than floating-point calculations to prevent precision errors that could misclassify instances (e.g.,  $23.99999 \neq 24$ ).

For unsolvable instances, we use a rejection sampling strategy: we randomly sample integer sets and retain only those for which the exhaustive solver proves the solution set is empty.

### A.4.2 Hamiltonian Cycle and Path Generation

The Hamiltonian Cycle problem asks whether a graph contains a closed loop visiting every vertex exactly once, while the Hamiltonian Path problem asks for a linear path visiting every vertex. Since these problems are NP-complete, we utilize a SAT-based verification pipeline to guarantee ground-truth labels.

---

**Algorithm 2** Hamiltonian Graph Generation

---

**Require:** Type  $T \in \{\text{Cycle}, \text{Path}\}$ , Node count  $N$

**Ensure:** A graph  $G = (V, E)$  with label

```
1: Function VERIFYSAT( $G, T$ ):
2:   Construct CNF formula  $\phi$  based on adjacency matrix of  $G$ 
3:   Add bijection constraints to  $\phi$ 
4:   if  $T == \text{Cycle}$ : Add closure constraint  $v_{N-1} \leftrightarrow v_0$ 
5:   return SAT-SOLVER( $\phi$ )
6: End Function
7: repeat
8:   Initialize empty graph  $G$  on  $N$  nodes
9:   if goal is Solvable:
10:    Create a random permutation  $P$  of vertices
11:    Add edges  $(P_i, P_{i+1})$  to form a base Path/Cycle
12:    Add random noise edges to increase density
13:   else if goal is Unsolvable:
14:    Select strategy  $\sigma \in \{\text{Disconnect}, \text{Bottleneck}, \text{DeadEnd}\}$ 
15:    Construct  $G$  satisfying  $\sigma$  (e.g., partition  $V$  into  $V_1, V_2$  with no edges between them)
16:    Add random noise edges strictly preserving  $\sigma$ 
17:     $IsFeasible \leftarrow \text{VERIFYSAT}(G, T)$ 
18:   until ( $IsFeasible$  matches goal)
19: return  $G$ 
```

---

**SAT Encoding.** We encode the existence of a path/cycle as a Boolean Satisfiability Problem. Let  $N$  be the number of vertices. We introduce boolean variables  $x_{v,i}$  indicating that vertex  $v$  occupies the  $i$ -th position in the sequence ( $0 \leq i < N$ ). The constraints are defined as follows: **Bijection** requires that  $\sum_v x_{v,i} = 1$  for all  $i$  and  $\sum_i x_{v,i} = 1$  for all  $v$ . **Adjacency** mandates that for all  $i \in [0, N - 2]$ , if  $x_{u,i}$  and  $x_{v,i+1}$  are true, then  $(u, v)$  must be an edge in  $E$ . Finally, **Cycle Closure (Cycle Only)** ensures that if  $x_{u,N-1}$  and  $x_{v,0}$  are true, then  $(u, v) \in E$ . We use the Minisat solver (via pysat) to determine satisfiability.

**Unsolvability Injection.** Instead of purely random sampling, we inject structural properties that inherently prevent Hamiltonian traversals. These include: **Structural Bottlenecks**, where graphs are generated with “bridge” nodes or articulation points that partition the graph into components that cannot be traversed in a single pass; **Degree Constraints**, where we inject nodes with degree  $< 2$  (dead ends) for cycles, or ensure the presence of  $> 2$  nodes with degree 1 for paths; and **Disconnectivity**, where we explicitly construct graphs with multiple connected components.

### A.4.3 Hitori Generation

Hitori is a logic puzzle played on an  $N \times N$  grid. The goal is to shade cells such that no number appears more than once in any row or column, shaded cells do not touch orthogonally, and all unshaded cells remain connected.

We model the puzzle as a Constraint Satisfaction Problem (CSP). We define binary variables  $x_{i,j} \in \{0, 1\}$  for each cell (1 denotes shaded). The key constraints are: **Uniqueness**, which requires that if a number  $v$  appears  $k$  times in any row/column, at least  $k - 1$  occurrences must be shaded; **Non-adjacency**, ensuring that for any adjacent cells  $u, v$ ,  $x_u + x_v \leq 1$ ; and **Connectivity**, verified via BFS to ensure all cells where  $x_{i,j} = 0$  form a single connected component.

Solvable instances are filtered to ensure a *unique* solution. Unsolvable instances are those where the CSP solver (combined with connectivity checks) returns a solution count of 0.

---

**Algorithm 3** Hitori Generation via CSP

---

**Require:** Grid size  $N$

**Ensure:** A validated Hitori grid  $G$

```
1: Function SOLVEHITORI( $G$ ):
2:   Initialize CSP solver  $P$ 
3:   Apply Row/Col constraints: Eliminate duplicates
4:   Apply Adjacency constraints: No adjacent black cells
5:    $\mathcal{S}_{local} \leftarrow P.getSolutions()$ 
6:    $\mathcal{S}_{valid} \leftarrow \emptyset$ 
7:   for each solution  $s \in \mathcal{S}_{local}$  do
8:     if CHECKCONNECTIVITY( $s$ ) then  $\mathcal{S}_{valid}.add(s)$ 
9:   end for
10:  return  $|\mathcal{S}_{valid}|$ 
11: End Function
12: repeat
13:   Generate random  $N \times N$  grid  $G$  with values  $\in [1, N]$ 
14:    $Count \leftarrow SOLVEHITORI(G)$ 
15:   if goal is Solvable and  $Count == 1$ :
16:     return  $G$  {Unique solution found}
17:   else if goal is Unsolvable and  $Count == 0$ :
18:     return  $G$  {Provably no valid configuration}
19: until Valid instance found
```

---

#### A.4.4 Maze Navigation Generation

The Maze Navigation task requires finding a valid path from a start position (S) to an end position (E) in a grid-based maze, where movement is restricted by walls.

**Verification Logic.** We employ Breadth-First Search (BFS) to determine solvability. BFS guarantees finding the shortest path if one exists. A maze is **Solvable** if a path from S to E exists, and **Unsolvable** if the set of reachable cells from S does not contain E.

**Construction Pipeline.** We first generate a complex solvable maze using a randomized Depth-First Search (DFS) algorithm, which ensures a spanning tree structure. To increase complexity, we selectively remove walls to introduce cycles and multiple potential paths, while validating that the solution remains unique or manageable using BFS.

To construct **Unsolvable Instances**, we employ a *Strategic Blockage* method rather than random wall placement. We analyze the solvable maze to identify all valid paths from S to E, and then select a *Critical Junction*—a coordinate  $(x, y)$  that lies on a valid path (or is shared by multiple paths). We place an obstacle (wall) at  $(x, y)$  and rigorously verify unsolvability using BFS. If the maze remains solvable (e.g., via a detour), we discard the instance or iteratively block remaining paths until connectivity is severed. This approach ensures that unsolvable mazes are structurally similar to solvable ones, often requiring the model to explore deep into the maze before realizing the path is blocked, thereby penalizing premature "give up" or hallucinated paths.

#### A.5 Hyperparameters

We implement our training pipeline using the ver1 (HybridFlow) framework (Sheng et al., 2025), which supports efficient reinforcement learning. The specific hyperparameters used for Group Relative Policy Optimization (GRPO) are detailed in Table 4. We set the group size  $G$  (denoted as `rollout.n` in ver1) to 12. Notably, we explicitly set `use_kl_loss=False`, meaning the KL divergence penalty term was disabled during optimization, relying instead on the probability ratio clipping to maintain policy stability. We differentiate the batch size for Qwen3-1.7B and Qwen3-4B to accommodate their respective memory footprints.

---

**Algorithm 4** Maze Generation with Strategic Blockage

---

**Require:** Dimensions  $W, H$ , Difficulty  $D$ **Ensure:** A maze grid  $M$  and label  $L$ 

```
1: Function VERIFY( $M$ ):
2:   return BFS( $M$ , Start, End)
3: End Function
4: repeat
5:    $M_{base} \leftarrow$  GENERATESOLVABLEDFS( $W, H$ )
6:   if goal is Solvable:
7:     return ( $M_{base}$ , VERIFY( $M_{base}$ ))
8:   else if goal is Unsolvable:
9:      $\mathcal{P} \leftarrow$  All paths in  $M_{base}$  from Start to End
10:    Select path  $P \in \mathcal{P}$  based on difficulty  $D$ 
11:    Select obstacle point  $o \in P$  (excluding Start/End)
12:     $M_{blocked} \leftarrow M_{base} \cup \{o\}$ 
13:    if not VERIFY( $M_{blocked}$ ):
14:      return ( $M_{blocked}$ , “Unsolvable”)
15: until Valid instance found
```

---

Table 4: Hyperparameter settings used in our experiments. We employ Group Relative Policy Optimization (GRPO) with the KL divergence penalty explicitly disabled to encourage broader exploration within the solution space.

Hyperparameter	Value
<i>General Optimization &amp; Generation</i>	
RL Algorithm	GRPO
Group Size ( $G$ )	12
KL Penalty Term	Disabled
PPO Mini-Batch Size	8
Sampling Temperature	0.6
Sampling Top- $k$	45
Max Prompt Length	2048
<i>Infrastructure</i>	
Hardware	8 $\times$ NVIDIA A100 GPUs
Tensor Parallelism (TP)	2
<i>Model-Specific Settings</i>	
<b>Qwen3-1.7B</b>	
Training Batch Size	32 $\times$ 12
Max Response Length	32,000
<b>Qwen3-4B</b>	
Training Batch Size	14 $\times$ 12
Max Response Length	32,000